Ocean Dynamics (2013) 63:691–707
DOI 10.1007/s10236-013-0622-4

The impact of silt trapping in large reservoirs on downstream morphology: the Yangtze River

Dirk Sebastiaan van Maren · Shi-Lun Yang · Qing He

Received: 5 March 2012 / Accepted: 1 May 2013 / Published online: 25 May 2013

Abstract The sediment load of the Yangtze River (China) is decreasing because of construction of dams, of which the Three Gorges Dam (TGD) is the best known example. The rate of the decline in sediment load is well known, but changes in the sediment grain size distribution have not been given much attention. The TGD mostly traps sand and silt while clay is flushed through the reservoir. A large amount of sand is available in the Yangtze River downstream of the reservoir, and therefore the pre-dam sand concentration is not substantially reduced. The availability of silt on the Yangtze River bed is limited, and it is expected that most silt will be removed from the riverbed within one to two decades. In order to evaluate the impact of the change in grain size distribution on the tidal flats of the Yangtze Estuary, a highly schematized tidal flat model is setup. This model broadly reveals that the observed deposition rates are exceptionally large because of the high sediment concentration, the abundance of silt, the seasonal dominance of waves (shaping a concave profile), and the offshore tidal asymmetry. The model further suggests that deposition rates will be limitedly influenced by reductions in clay or fine silt but strongly impacted by reductions in median to coarse silt. The response of the downstream morphology to reservoir sedimentation therefore strongly depends on the type of trapped sediment. As a consequence, silt-dominated rivers, such as the Yangtze River and the Yellow River may be more strongly impacted than sand-dominated systems.

Keywords Tidal flats · Morphodynamics modeling · Silt · Reservoir siltation · Three Gorges Dam · Yangtze River

Responsible Editor: Andrew James Manning

This article is part of the Topical Collection on the *11th International Conference on Cohesive Sediment Transport*

D. S. van Maren (✉)
Deltares, PO Box 177, 2600, MH Delft, The Netherlands
e-mail: bas.vanmaren@deltares.nl

D. S. van Maren
Faculty of Civil Engineering and Geosciences,
Delft University of Technology, Delft, The Netherlands

S.-L. Yang · Q. He
State Key Laboratory of Estuarine and Coastal Sediment Dynamics and Morphodynamics, East China Normal University, Shanghai 200062, China

1 Introduction

River deltas are inhabited by over 60 % of the world population, and are, consequently, of paramount agricultural and economical importance. More than 50 % of the world population lives in Asia, most of which on the large deltas of the Ganges, Brahmaputra, Irrawaddy, Chao Praya, Mekong, Pearl, Yangtze, Yellow River, and Red River (Saito 2001). The ensuing pressure on space makes land protection and reclamation a key issue, thus sediment is a valuable resource (e.g., Chen et al. 2006). However, the sediment load of most major river systems is decreasing due to trapping in reservoirs (e.g., Vörösmarty et al. 2003; Walling 2009). In addition to this reduction in sediment load, river deltas are threatened by sediment compaction due to removal of oil, gas, and water from the delta's underlying sediments, floodplain engineering, and rising global sea level (Syvitski et al. 2009). The impacts of a dam on the river downstream in terms of hydrology and morphology are determined by a complex mix of variables that includes the patterns of release of water through the dam and the characteristics of the downstream channel (Chen et al. 2010). Predictions on the effect of reservoir siltation on the downstream river or delta morphology is primarily based on reduction of the total sediment load, such as Yang et al. (2003a). However, river deltas are composed of sand, silt and clay, with a spatial segregation reflecting the sediment availability in the river basin, the transport capacity of the river, and the reworking capacity of the receiving basin. Typically, the

coarsest sediment (transported as bed material load) is deposited in (or within a short distance from) the river mouth, while the percentage of sand decreases rapidly in the seaward direction. The offshore deltafront and the prodelta are fine grained, built by the finest sediment fraction (transported as washload).

Depending on its size and operational strategies, a reservoir typically traps coarse sediment while a substantial part of the fine-grained sediment may be released (Xu 2007). In large river systems with a large sediment availability and relatively coarse sediment, the equilibrium sediment concentration may be re-established in the reaches between the reservoir and the delta. The impact of sediment trapping on coarse-grained sediment supply to the river mouth is then probably limited. It should be realized that although these systems are not strongly impacted by reservoir siltation, their morphology may be strongly influenced by changes in flood frequency and magnitude. Very fine-grained systems, on the other hand, may also be only influenced to a limited extent, because a large part of the clay fraction is flushed through the reservoirs. Sediment of intermediate size may be most strongly impacted. A large amount of this sediment (mainly silt and fine sands) may be trapped at ratios comparable to sand (nearly 100 %). Since silt has a larger transport capacity than sand (with concentrations typically several grams per liter to tens of grams per liter), the fine-grained sediment available in the downstream river bed can be rapidly removed. Furthermore, the amount of silt in the downstream river bed is probably limited (typically the flow velocity is sufficiently large to keep sediment in suspension) and therefore silt trapping will lead to a depletion of silt in the downstream river delta. River deltas tend to be more fine-grained than the upstream river, and silt often is the dominant sediment type. As a result, it is the reduction of the intermediate fraction that may have the greatest impact on downstream delta morphology, and rivers carrying fine-grained sediment which is sufficiently coarse to be trapped in reservoirs will be most impacted. Although depending on the hydrodynamics in the reservoir and the downstream river, this typically concerns fine sands and silts. Silt-laden rivers are most common in China, with the Yangtze River and the Yellow River as the best known examples. More than half of the world's large dams commissioned since 1950 have been built in China (Fuggle and Smith 2000) and as a result, the sediment dynamics of the silt-laden rivers in China are especially impacted by reservoir siltation.

The mouth of the Yangtze River is composed of extensive and rapidly accreting tidal flats and salt marshes which provide ecologically important habitats but also enable land reclamations in an economically rapidly developing region (including Shanghai and its port). It is expected that the accretion rate of the flats will decrease or even reverse to erosion (Yang et al. 2005, 2011). However, these established relations between sediment load and tidal flat dynamics are highly empirical and do not provide further insight in the role of sediment segregation. Suspended sediment dynamics, and the resulting morphological change, on intertidal flats is complex and strongly linked to the sediment type available. The rapid accretion rates of the Yangtze flats may be related to abundance of silt, which has sediment properties (settling velocity, critical shear stress for erosion) that promote high net accretion rates on intertidal areas (van Maren and Winterwerp 2013). Therefore a reduction in the silt fraction may more strongly impact the intertidal flats than only a reduction in the total sediment budget would suggest. However, the impact of such a changing sediment supply on the tidal flats is difficult to determine from field observations because of the large natural variability of processes (discharge and wave events) and large amount of human interferences (local land reclamation and large-scale constructions elsewhere in the estuary). Additionally, insufficient data on sediment size distribution is available to derive quantitative relationships between sediment fractions and intertidal flat dynamics. Numerical modeling provides an alternative in which such individual processes can be analyzed and future scenarios evaluated. The aim of this study is to examine the influence of a changing sediment size distribution and sediment load on accretion rate, using available data and a cross-shore profile model. This paper is organized as follows. The Yangtze River is described in Section 2 and the methodology in Section 3. Results are presented in Section 4 and discussed in Section 5.

2 Study area: the Yangtze River and estuarine tidal flats

2.1 The Yangtze River

The Yangtze River has a catchment area of 1.8×10^6 km^2 and discharges around 30×10^3 m^3/s. The long-term (1950–2000) average sediment loads at Yichang (downstream of the present-day Three Gorges Dam (TGD)) and at Datong (tidal limit) are 501 and 433 Mt/y, respectively (Xu and Milliman 2009). Although some sediment is deposited between Yichang and Datong (Yang et al. 2007a), about 50 % of the sediment is deposited in the Yangtze Estuary (Yang et al. 2008) while the remaining sediment is discharged into the East China Sea (Fig. 1).

The sediment load of the Yangtze River has been steadily decreasing in the past decades (Yang et al. 2007b; Xu and Milliman 2009; Yang et al. 2011; Li et al. 2011) (see Fig. 2a). Dam construction within the Yangtze River basin started in the 1950s, and sedimentation in the reservoirs reduced the sediment load at Yichang from 530 (1950–1985) to 410 Mt/year (1986–2002) (Yang et al. 2006). This decrease accelerated after the commissioning of the TGD: during its first stage of deployment (2003–2005), 64 % of sediment entering the Three Gorges Reservoir was trapped (Yang et

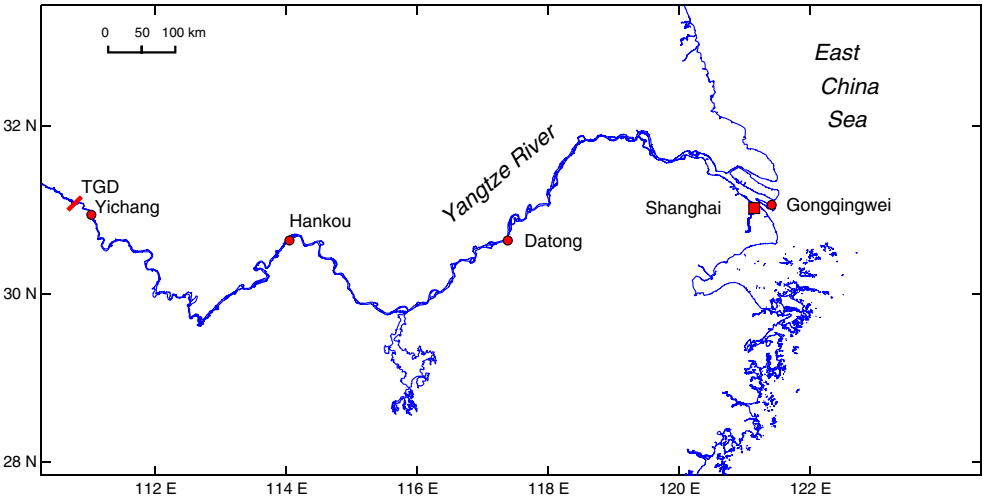

Fig. 1 Yangtze River downstream of the Three Gorges Dam (*TGD*) with the main hydrological stations Yichang, Hankou, Datong, and the water-level station Gongqingwei in the Yangtze Estuary

al. 2007b). Since then the water level of the reservoir has been raised from 135 m in 2005 to 156 m in 2006 and 175 m in 2008, and as a result, more than 80 % of sediment entering this reservoir is now trapped (Zhang 2011). The channel downstream of the TGD reverted from an accretion rate of ~90 Mt/y between the mid-1950s and mid-1980s to an erosion rate of ~60 Mt/y after closing of the TGD (Yang et al. 2011). The sediment concentration immediately downstream of TGD has decreased from >1 g/l before 1990 to ~0.1 g/l (Fig. 2b). Further downstream, the sediment concentration at Datong decreased from approximately 0.5 g/l to 0.2 g/l. Within the Yangtze estuary and adjacent coastal sea, the surface sediment concentration has become 20–30 % lower in the past 10–20 years (Li et al. 2011).

Especially compared with scientific attention paid to the impact of the TGD on sediment loads (see references above), little or no scientific studies have addressed the changing sediment size distribution. Before construction of the TGD, the yearly averaged median grain size (D_{50}) of the suspended load of the Yangtze was ~10 μm (Fig. 2c). After closure of the TGD, the yearly average D_{50} immediately downstream of the dam (Yichang station) reduced to 4.4 μm on average in 2003–2010 (Fig. 2c). This low D_{50} implies that mainly clay and very fine silt is released from the TGD: only during flushing of larger floods coarser sediment (coarse silt and sand) may be released. Hence, most silt presently delivered to the Yangtze Estuary is probably eroded from the downstream river bed. Assuming that silt can be

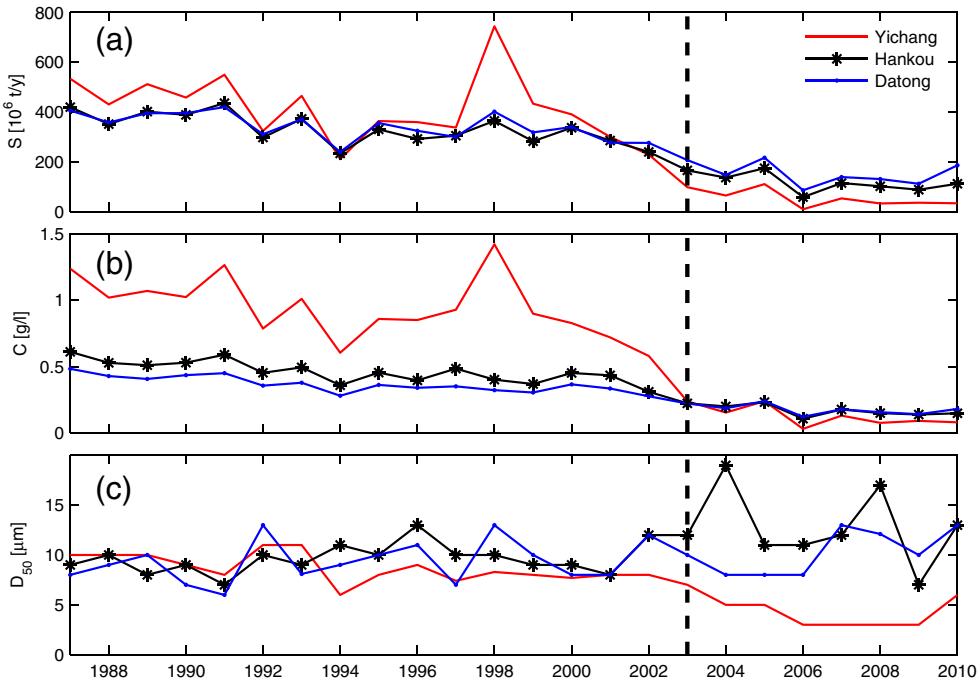

Fig. 2 Sediment load (**a**), sediment concentration (**b**), and grain size (**c**) measured at Yichang, Hankou, and Datong, respectively (see Fig. 1 for locations). The *black dashed line* indicates the impoundment of the TGD

eroded from the active layer of the river bed, the silt availability can be estimated from the cross-sectional width, the river length, and the silt content. The river bed is primarily composed of medium and fine sand (grain size of 100 to 400 μm): coarse sand occurs locally and silt is more prevalent in the river mouth area (Wang et al. 2009; Luo et al. 2012). The silt content varies from 4 to 50 % throughout the downstream river and estuary but is typically less than 10 % (Wang et al. 2009; Luo et al. 2012). With a length of 1,700 km (from the TGD to the estuary head), an average width around 1,000 m, and a silt content of 10 %, 170 million m^3 or 220 million ton (the bulk density is ~1,300 kg/m^3) can be winnowed from the top meter of the river bed. Since this is equivalent to 4 years of erosion estimates (e.g., Yang et al. 2011), it is expected that silt will be rapidly (within one to two decades) eroded from the river bed downstream of the TGD.

2.2 The Yangtze estuary and tidal flats

The Yangtze estuary is composed of four main branches intersected by islands. The seaward end of the estuarine islands and the coastline south of the Yangtze Estuary is bordered by extensive tidal flats facing the East China Sea (Fig. 3); the widest are the tidal flats east of Chongming Island and in the Jiuduansha shoal. For example, the tidal wetland in Eastern Chongming is 8 km wide, of which the upper 2.5 km is covered with vegetation (Yang et al. 2008; Yang et al. 2011). The spring tidal range is 3.5 m near Chongming Island and Jiuduansha. There is a pronounced seasonal variation in the wave climate because of the occurrence of typhoons from May to November. The annual mean wave height is 1 m (Yang et al. 2008), but field observations during the 1999 typhoon season revealed that a maximum wave height of 2.5 m on the inner shelf off the Yangtze River Delta was exceeded seven times (Fan et al. 2006). These waves will further attenuate when traveling deeper into the estuary and therefore the Yangtze Estuary can be considered a low energy environment despite the occasional typhoon passage (Chen et al. 1985).

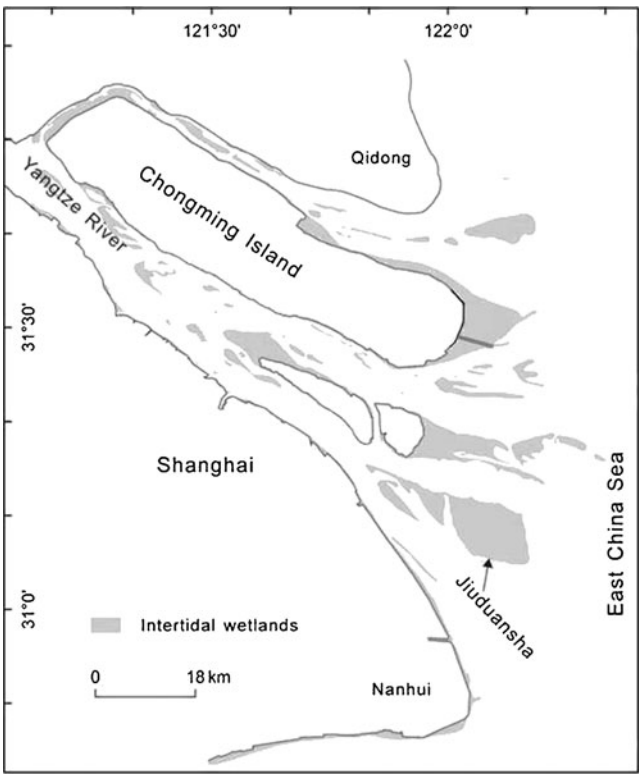

Fig. 3 Tidal flats in the Yangtze estuary. The Chongming flats are east of Chongming island (with the location of the transect in Fig. 4 in *grey*). The Luchaogang and Nanhui flats are close to Nanhui, although their aerial extent is presently very limited due to recent land reclamations

The suspended sediment concentration in the Yangtze estuary is typically several hundreds of milligrams per liter (He et al. 2003), increasing in the downstream direction towards an Estuarine Turbidity Maximum (ETM) located at the transition from the estuary to the East China Sea (around the 10-m depth contour). A full year of daily surface sediment concentrations collected east of Chongming Island (Sheshan station, at the 5-m depth contour) shows that the average suspended sediment concentration is 0.42 g/l, with winter concentrations about twice the summer concentrations (Chen et al. 2003). Spring tide sediment concentrations are only 10–20 % higher than neap tide concentrations (see He et al. 2003). The sediment concentration in the intertidal zone is much larger, frequently exceeding 1 g/l (see Yang et al. 2003b). Although the median grain size of the primary particles suspended in the water column is typically 5–12 μm, the size of the flocs is an order of magnitude larger: estimates of Guo and He (2011) (50–120 μm) agree fairly well with Shao et al. (2011) (20–150 μm). These flocs originate from the freshwater region of the Yangtze, in which similarly large flocs were observed (Guo and He (2011)). The sediment settling velocity within the estuary typically ranges between 0.2 and 2 mm/s according to He et al. (2004) and Guo and He (2011), although Shao et al. (2011) computed settling velocities about two times larger.

The tidal flats are dominantly composed of silt: the median grain size is around 30 μm near Luchaogang (see Fig. 5) but is more variable in Eastern Chongming (Yang et al. 2008) and Jiuduansha (Yang 1999). More detailed field investigations of the tidal flats by Te Slaa et al. (2013) reveal that the flats bordering the main outflow channel of the Yangtze (south of Chongming Island) have clay percentages of less than 10 % (either in aggregate form or as primary particles). Only the northern flats of Chongming, which is more strongly influenced by marine sediments, contain more clay: typically 10–25 %. All flats are dominated by silt, typically forming more than 70 % of the deposit. Clay particles do become more

abundant in the marshes bordering the flats on their landward side (more than 30 %; Yang 1998): the division between permanent vegetation and bare tidal flat occurs around 0.5 m above mean sea level (MSL).

The Yangtze tidal flats have been rapidly accreting in the seaward direction: the coastline used to migrate seaward at an average rate of several tens of meters per year (Yang et al. 2001; Fan and Li 2002), and up to 300 m/year in Eastern Chongming (Yang et al. 2001) (Fig. 4). However, in recent years the accretion rates have strongly decreased and locally even reversed to erosion (Yang et al. 2005) (Fig. 4). The tidal flats on the Yangtze have a pronounced annual variation in erosion/deposition (e.g., see Fig. 5). Deposition occurs in the upper salt marsh during the storm season (May/June to November), during which the bare tidal flat is eroded (Jiuduansha flats: Yang 1999; Nanhui flats: Fan and Li 2002, 2006; Yang et al. 2003b; Chongming flats: Yang et al. 2008). Erosion will occur when the offshore wave height exceeds 1.6 m (Fan et al. 2006). These conditions are typical for swells generated by typhoons (including distant typhoons): local wind-generated waves appear to play a minor role for the onset of erosion (Fan et al. 2006). From December to May, the bare tidal flats accrete (typically several decimeters per season; see, e.g., Fig. 5), with fine-grained sediment (30 μm; see Fig. 5). During calm periods, the vertical accretion rates are typically 2 to 5 mm/tidal cycle, deposited during the flood tide (and occasionally during ebb tide; Fan and Li 2002). Accretion rates are highest during spring tides (~2 cm/day; see Fig. 6). The daily deposition rate in Fig. 6 exceeds the monthly bed level changes in Fig. 5 because sediment is continuously reworked: the short-term (~months) preservation potential of the daily accumulation is about 25 % (Fan and Li 2002). These high deposition rates may result from the proximity of the ETM of the Yangtze, which is located near the river mouth.

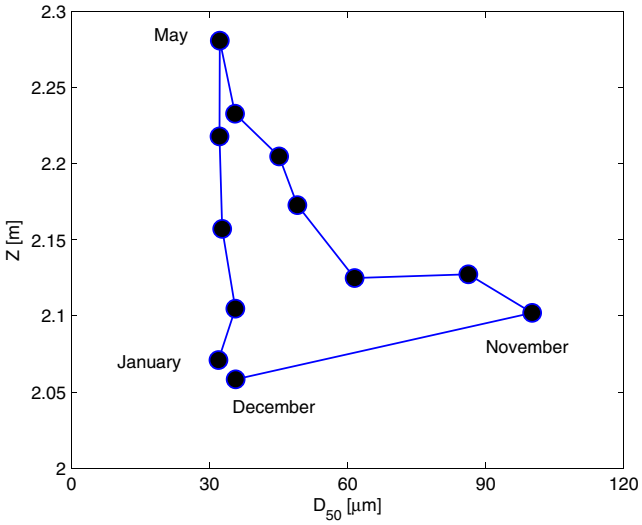

Fig. 5 Relationship between monthly mean grain size and bed level (above LAT) on the middle flat of Luchaogang in 2003. From Yang et al. (2008)

3 Methods

3.1 Introduction

Complex process-based numerical models have become increasingly used tools to analyze river delta morphodynamics (i.e., Edmonds and Slingerland 2009; Geleynse et al. 2011). Even though such models can be used to compute an impact of dams on downstream morphology (Kuang et al. 2013), they lack the spatial and vertical resolution to accurately resolve the complex processes related to intertidal flat sedimentation. These processes are much better represented in cross-shore profile models, such as those used by Roberts et al. (2000), Pritchard et al. (2002), Pritchard and Hogg (2003), and van

Fig. 4 Cross-shore profile of the tidal flats east of Chongming Island (see Fig. 3 for location)

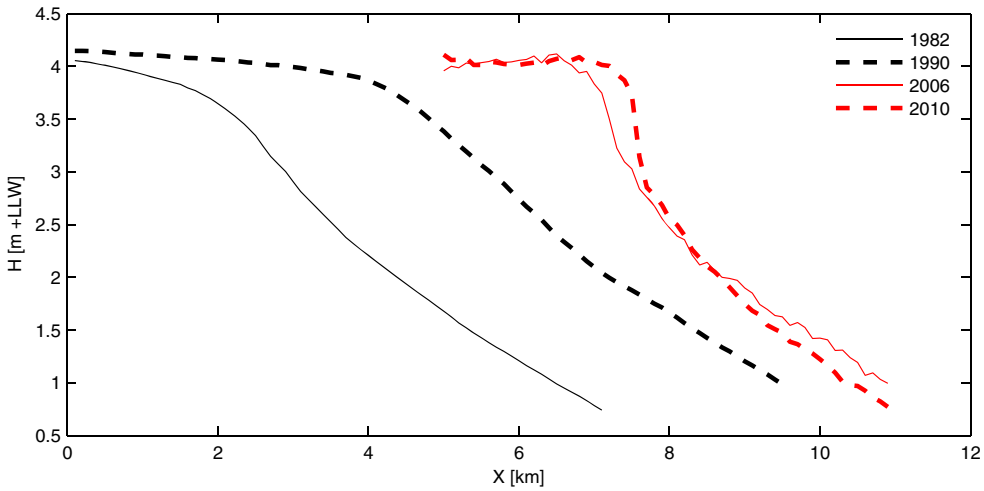

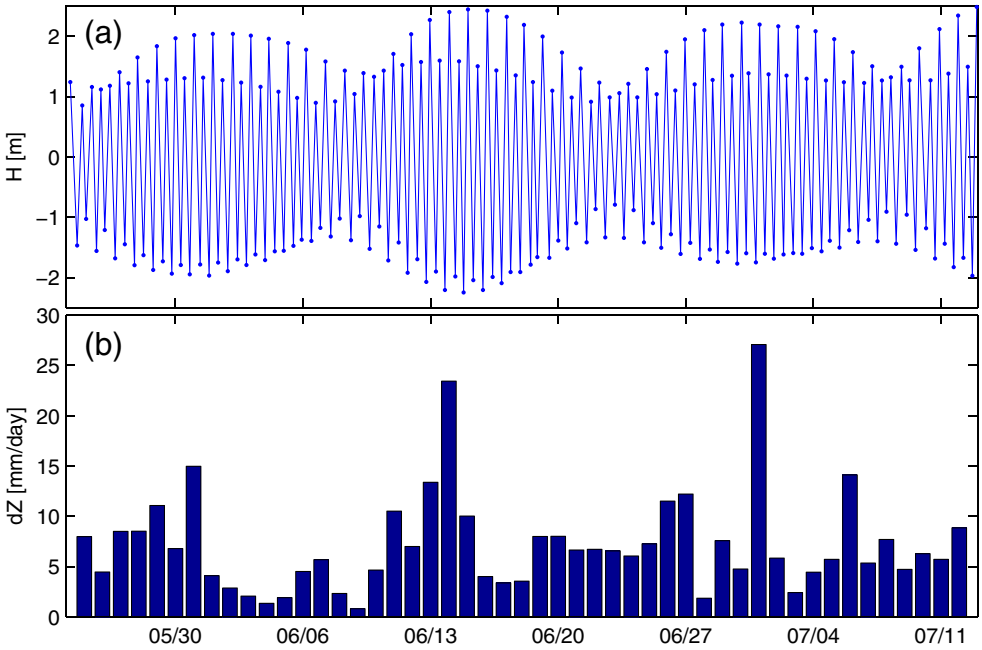

Fig. 6 Water level (**a**) and daily deposition rate (**b**) at Luchuogang tidal flat, in 1999. The daily deposition rate is computed from the tidal couplet thickness at two sites presented by Fan and Li (2002)

Maren and Winterwerp (2013). A model with relatively complex physical processes that reproduces the essential transport processes can be utilized as a numerical laboratory to experiment with the relative role of dominant processes. Since we aim to reproduce tide-induced sediment deposition on tidal flats, we use a multi-fraction model (mainly consisting of silt fractions) with a stratigraphy module for the bed development, and a large vertical resolution to model suspended sediment transport. Although the validity of such a profile models is restricted in case of strong alongshore currents or complex geometries, it does provide valuable insight into the importance of hydrodynamic and sedimentary processes. Despite complex physical process formulations, their simplified geometries do imply that model results should be interpreted carefully.

Net deposition on tidal flats depends on erosion and deposition processes. Generally, tidal currents in combination with settling and scour lags result in deposition. Resuspension by waves generates strong cross-shore sediment concentration gradients, which, in combination with diffusion by tidal currents, generates offshore transport, and thereby erosion. Numerical modeling of wave-induced erosion is complex because of uncertainties in offshore wave heights, dissipation of wave energy over the tidal flat, and contributions of the wave-induced shear stress on resuspension rates. The net erosion or deposition resulting from the combined tidal and wave-induced processes is therefore difficult to predict. On the tidal flats in the Yangtze Estuary, there is a clear distinction between periods in which erosion dominates and periods when deposition prevails (see Fig. 5). To identify the effect of changes on reservoirs on tidal flat deposition rates, we focus on the period in which deposition prevails. We only consider cross-shore tidal flow since on most tidal flats, alongshore flows dominate the sediment transport in deeper water (Le Hir et al. 2000). For the flats in the Yangtze estuary, this implies that the model is mainly valid on the seaward-facing flats and not so much on the flats bordering the river channels (which also experience little or no net deposition).We use a relatively short cross-sectional area (10 km in the offshore direction) in order to prescribe simple hydrodynamic forcing.

3.2 Model description

The tidal flats in the Yangtze are characterized by a concave profile with gradients of 0.0005 at the lower intertidal zone up to 0.002 at the upper intertidal zone (e.g., Fan et al. 2006; Yang et al. 2008) (see also, Fig. 4). The tidal range is approximately 4 m during spring tides (Fig. 6a). We schematize these conditions in a 2DV cross-shore profile model based on the Delft3D model to simulate tide-induced transport of fine sediment. Delft3D solves the unsteady shallow water equations in two or three dimensions under the hydrostatic pressure assumption and computes sediment transport and morphological update simultaneously with the flow (see Lesser et al. 2004) for a description and validation. This model has been successfully applied to reproduce sediment transport and deposition patterns in the fine silt range and at associated typical high sediment concentrations (see, e.g., van Maren 2007; van Maren et al. 2009a; Hu et al. 2009; Ying et al. 2012). We prescribe a cross-shore profile with a gradient of 0.002 at high water (HW), decreasing linearly to 0.0005 at 5 km in the offshore direction. Further seaward the bed level decreases another 5 km in the seaward direction, using a constant gradient of 0.0005 (Fig. 9a). These

conditions are typical for most of the seaward facing flats in the Yangtze (Nanhui, Jiuduansha, and Eastern Chongming). The model is forced with a water-level variation measured at Gongqingwei (in-between Chongming and Jiuduansha (see Fig. 10a)). The horizontal grid cell size is 100 m in the cross-shore direction, and the vertical grid consists of 20 vertically uniform σ layers.

The sediment dynamics are computed with a morphodynamics model based on the Partheniades equation for erosion E and a permanent deposition flux D:

$$E_i = M_i\left(\tau - \tau_{cr,i}\right) \Big/ \tau_{cr,i}$$

$$D_i = w_{s,i} C_i$$

Here, M is the erosion parameter (in kilograms per square meter per second), w_s the settling velocity and C the concentration (in kilograms per cubic meter). The subscript i denotes the sediment fraction. The model simulates six fractions: a clay fraction (sediment diameter D=2 μm), three fine silt fractions (D=6, 11, and 18 μm), medium silt (D=33 μm), and coarse silt (D=58 μm). The bed evolution is computed with a dynamic multilayer bed module, consisting of up to 100 vertical layers, each 5 mm thick. The amount of active layers depends on the amount of sediment in the bed: the initial sediment bed is empty. When the amount of sediment deposited exceeds the layer thickness (5 mm), the bed layer in that specific grid cell becomes an inactive part of the bed and a new layer is generated at the water-bed interface. Erosion/deposition is computed per fraction i for the upper layer only, with erosion rates depending on the sediment availability of this upper layer. When the upper layer is fully eroded, sediment in the layer below becomes (again) available for erosion. This implies that finer sediment deposits in deeper layers can be armored by sediment less easily eroded in upper layers (armouring).

There is clear evidence for increasing settling velocity in the Yangtze River due to flocculation processes (Guo and He 2011; Shao et al. 2011). Flocculation will therefore play a (possibly important) role in sedimentation processes. However, in the current model setup, flocculation is not accounted for. Firstly, this is because the sediments on the Yangtze tidal flats (excluding the marshes) are strongly dominated by silt and fine sand (Te Slaa et al. 2013). Even though clay particles or organic matter influence silt dynamics through flocculation, we assume flocculation processes to be of secondary importance. Secondly, we aim to relate the relative importance of certain fractions to deposition rates, and understand the physical mechanisms responsible for deposition. Establishing such relationships is more straightforward without a flocculation model. Therefore, we model all sediment fractions with constant settling velocities based on Stokes' law (as in Fig. 7). The range in settling velocity of these primary particles (between 0 and 4 mm/s) is similar to observations by He et al. (2004), Guo and He (2011), and Shao et al. (2011).

The sediment concentration imposed on the boundaries is 0.4 g/l (based on the measurements reported by Chen et al. 2003 and He et al. 2003). Although these measurements were done near surface, we prescribe the concentration depth averaged, implying we underestimate the actual sediment supply. This total sediment concentration is distributed among the various sediment fractions according to their estimated distribution in the Yangtze River. We know that the long-term average grain size D_{50} of suspended sediment in the Yangtze River is around 10 μm (see Fig. 2). However, the median grain size in the Yangtze estuary is variable, and the particle size distribution (PSD) even more. Even for a long-term-averaged constant D_{50} (10 μm), the distribution around the median may play an important role in tidal flat dynamics. In order to evaluate the effect of this (unknown) variation of the grain size distribution around the mean, we have defined 3 PSD's (see Fig. 8). Distribution 1 is the most realistic estimate, while distribution 2 consists of a relatively large amount of fine silt, but has less clay and coarse silt. In contrast, distribution 3 has a relatively large amount of clay and coarse silt, and relatively less fine silt. These sediment distributions should not be interpreted as a typical variation of PSD's in the Yangtze Estuary, but provide a bandwith of PSD's for D_{50}=10 μm.

The critical shear stress for erosion decreases from 0.1 Pa for coarse silt to 0.03 Pa for very fine silt according to the Shields curve (Fig. 7). However, this Shields curve is based on particles with a grain size equivalent to sand and larger and is not valid for sediment particles in the silt range. Laboratory experiments by Roberts et al. (1998) revealed that the critical erosion shear stress of silt depends on the degree of compaction, which could be explained by shear dilatancy effects (Mastbergen and van den Berg, 2003; van Maren et al. 2009b). Van Rijn (2007) proposed an alternative to the Shields curve for silt particles, with a factor γ representing the degree of compaction (see van Rijn 2007 for more details). This suggests (see Fig. 7) that 0.1 Pa is a reasonable estimate for the critical shear stress of all the modeled sediment fractions. This agrees with the critical shear stress computed by Shi et al. (2011) from data collected in Eastern Chongming.

4 Results

4.1 Model calibration

The aim of our model is to reproduce typical sediment dynamics in the Yangtze River intertidal flats. Therefore

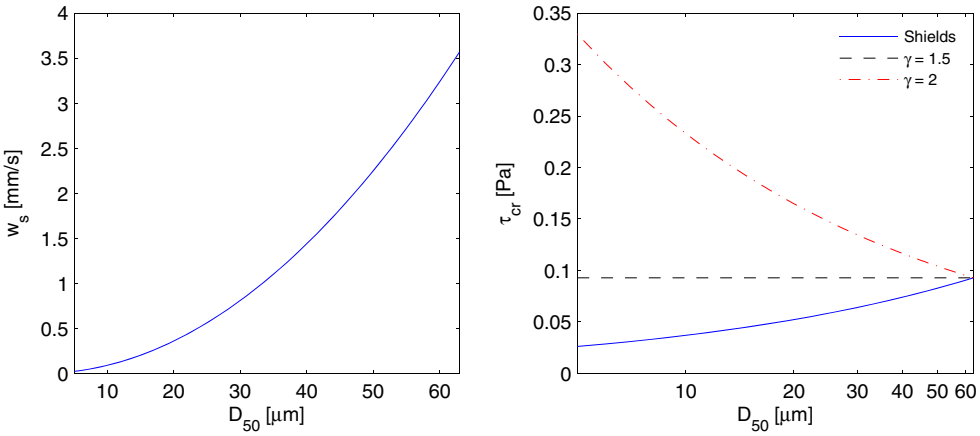

Fig. 7 Stokes' settling velocity of primary particles in the silt range (temperature 20 °C; *left panel*), and the critical shear stress τ_{cr} for erosion according to Shields, and with the modification by van Rijn (2007) using γ=1.5 and γ=2.0 (*right panel*)

the model should reproduce the typical sedimentation rates, the spring–neap variation thereof, and the typical grain size of the sediment deposits.

The highest deposition rate (in the cross-shore direction) on the intertidal flats is 40 cm in 90 days (see Fig. 9).This is in line with observations, typically several dm per season (Fig. 5). The grain size of the modeled intertidal flat deposits decreases from 60 μm at the lower flat to 20 μm on the upper flat. This trend is in line with observations on various flats in the Yangtze estuary (Yang et al. 2008). Interestingly, the deposition of fine-grained sediments on the upper flat is often associated with vegetation prevalent on the upper flat. Our model results show that this cross-shore grain size gradient is at least partly caused by tidal processes as well. The effect of the sediment distribution (i.e., the spread around the D_{50} of 10 μm) on average deposition rates, but also on the cross-shore distribution of the deposits (reflected in the proportional distribution over the higher and lower intertidal zone, see also Fig. 13) is low. This implies that the absence of detailed information on grain size distribution only marginally influences our model results.

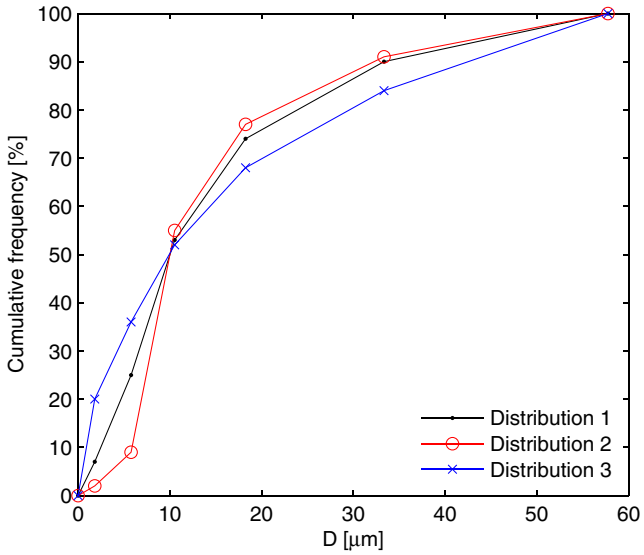

Fig. 8 Sediment distributions 1, 2, and 3, all with a median grain size of D_{50}=10 μm. Distribution 2 is more abundant in sediment with grain size D=10 μm, whereas distribution 3 has relatively less sediment with D=10 μm

The modeled spring–neap variation of net sediment deposition (Fig. 10) agrees fairly well with the observed spring neap variation in daily deposition rates (Fig. 6). The model seems to overestimate spring tide deposition rates relative to neap tide deposition rates, when compared with observations. However, this may be due to lower preservation potential of neap tide deposits: 75 % of the daily deposition rate (as provided by Fig. 6) is later reworked (Fan and Li 2002). Spring tide currents typically erode neap tide deposits (which are often more fine-grained and easier to erode) and mainly spring tide deposits remain preserved (as in Fig. 10). Model limitations, which may also partly contribute to disagreements between model and data, will be discussed in more detail in Section 5.1.

The modeled flow velocities peak at 0.4 m/s, which is lower than the flow velocities observed on the Chongming island flats (typically around 0.5 m/s; see Yang et al. 2008 and Shi et al. 2012), mainly because alongshore flow is excluded. There is a pronounced asymmetry in the flow velocity, with higher flood flow velocities than ebb flow velocities. This asymmetry results from the offshore water levels. In a semi-diurnal regime such as the Yangtze estuary, the asymmetry of the tide is determined by the amplitude ratio of M_2/M_4, and the phase difference between M_2 and M_4 $\left(2\phi_{M_2}-\phi_{M_4}\right)$. Standard harmonic analysis using T-Tide (Pawlowicz et al. 2002) revealed that the water-level amplitude of M_2, S_2, and M_4 is 115, 49, and 15 cm. The phase difference $\left(2\phi_{M_2}-\phi_{M_4}\right) = 72$, implying a flood-dominant asymmetry with a faster rise then fall of the tide (see, e.g., Friedrichs and Aubrey 1988). For these conditions, flood flow velocities are large than the ebb flow velocities.

The modeled sediment concentrations sharply increase in the landward direction, from several 100 mg/l at the offshore boundary up to 20 g/l in the intertidal area (Fig. 11c is cut-

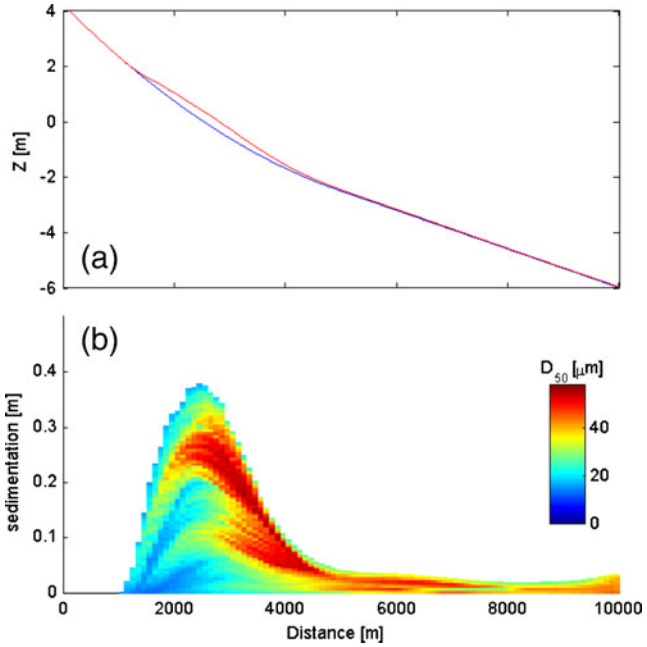

Fig. 9 Modelled cross-shore profile (**a**), with Z relative to MSL at the beginning (*blue*) and after 90 days (*red*) and sediment composition of the deposited sediment (**b**), for sediment distribution 1

off at 6 g/l). Sediment concentrations of several g/l are commonly observed on the various flats in the Yangtze estuary (e.g., Yang et al. 2003b; Li and Yang 2009). Even though the sediment concentrations increase in the landward direction to an optimum in the upper intertidal zone, the instantaneous sediment transport rates are more spatially uniform (Fig. 11d). This is because the increase in sediment concentration is compensated by a decrease in water depth (suspended sediment transport scales approximately linearly with the water depth and sediment concentration). The cumulative transport, however, clearly decreases in the landward direction (Fig. 11e). This is the result of trapping of particles at HW, resulting in rapid accretion rates (Fig. 11f).

Summarizing, the model qualitatively reproduces the net and spring–neap variation in deposition rates and grain size distribution, as well as observed sediment concentrations. The sensitivity of the modeled deposition rate to the unknowns in the actual grain size distribution is low. Therefore the model is subsequently utilized to evaluate changes in offshore sediment supply on tidal flat deposition rates and patterns.

4.2 Sediment scenarios

The degree of sediment transport reduction due to a dam depends on the timescale (effect of all dams or only one dam, i.e., several decades or one year), and the size of the area of interest (directly below the dam or 1,000 km downstream). From 1950 to 2002 the sediment of the Yangtze decreased with 23 % (Yang et al. 2006), but presently 80 % of all incoming sediment is trapped in the TGD (Zhang 2011). It is expected that also in the Three Gorges Reservoir a new equilibrium will be reached in which sedimentation rates will decrease again. Therefore we assume a sediment load reduction of 25 %.

There is no sufficiently quantitative information available on how this reduction influences the sediment size distribution, not in the Yangtze River itself, but even more not how the PSD has already changed or will change in the Yangtze

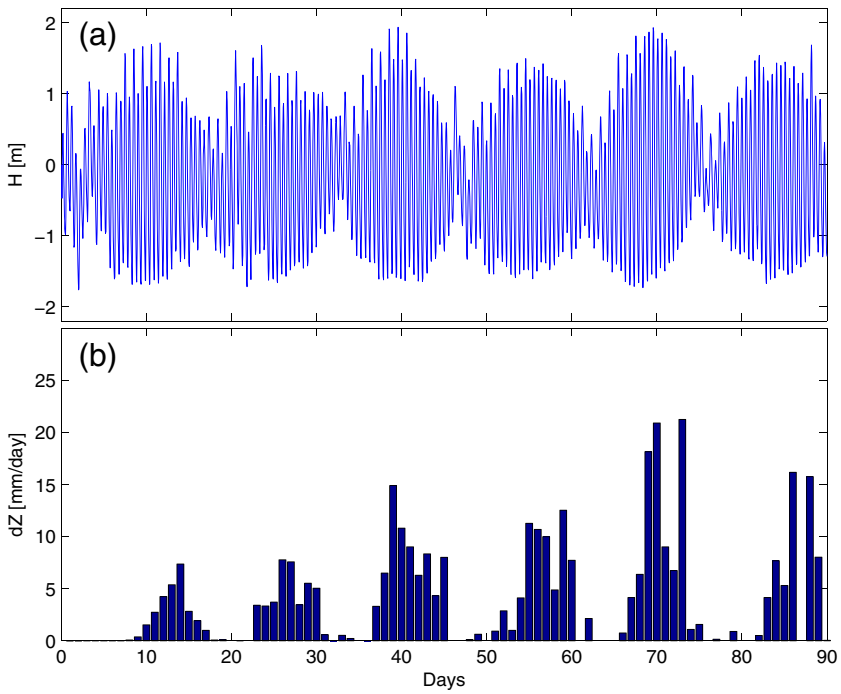

Fig. 10 Water levels measured at Gongqingwei, close to Chongming Island (**a**) and daily deposition rates on the intertidal one (**b**) modeled with sediment distribution 1

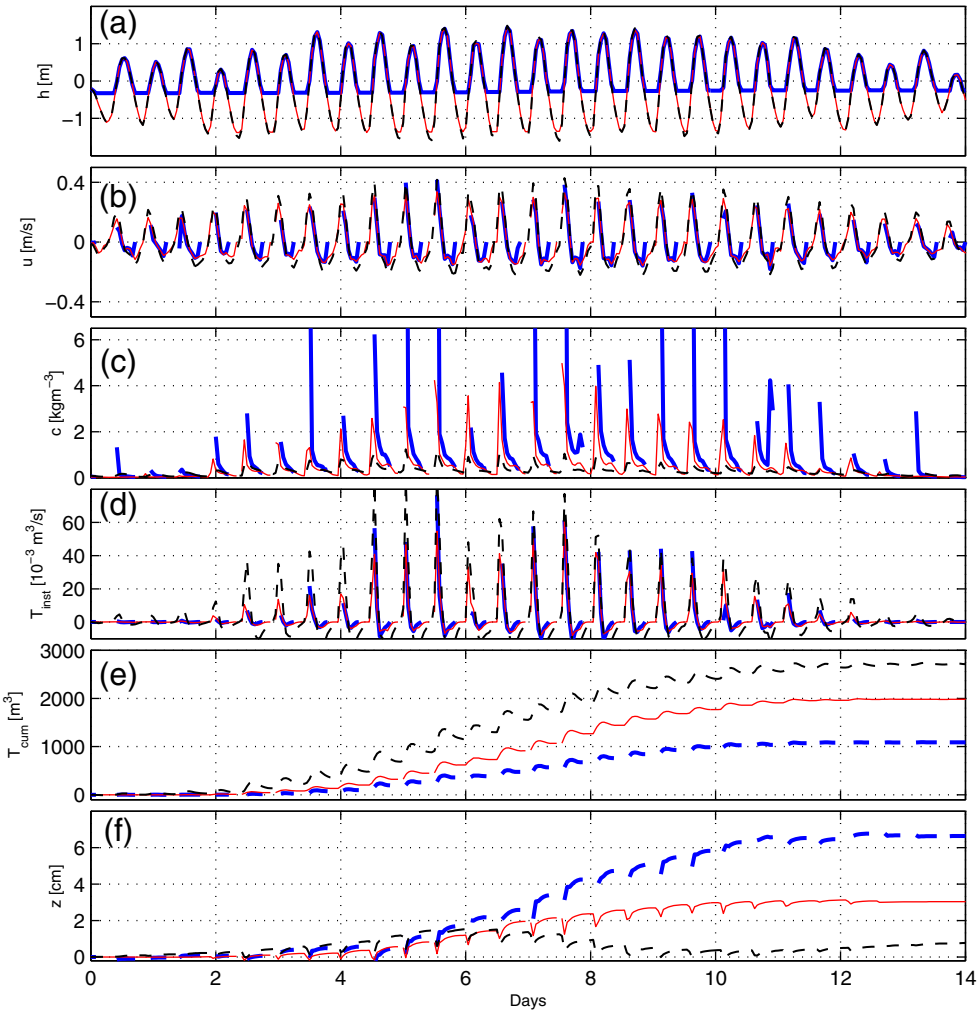

Fig. 11 Water level (**a**), depth-averaged flow velocity (**b**), depth-averaged sediment concentration (**c**), instantaneous transport (**d**), cumulative transport (**e**), and bed-level change (**f**) at 1 km from the seaward boundary (black dashed), just seaward of the LW line (X≈3,800 m, in *red*), and in the upper tidal flat (X≈2,800 m, in *blue*; X is shown in Fig. 9), using sediment distribution 1. Transport and flow velocity are defined positive in the upflat direction

Estuary. As an alternative, we do a sensitivity analysis on the PSD by systematically reducing the sediment availability in a certain sediment size fraction. We previously defined six sediment fractions. Based on these six fractions, six scenarios (A–F) are defined, with each scenario impacting a specific sediment fraction. For scenario A, sediment is removed from the finest fraction (D=2 μm) while for scenarios B–F progressively coarser sediment is removed. For fractions constituting less than 25 % of the total sediment load, the remaining reduction is evenly distributed among a coarser and finer fraction. Since especially the coarser fractions are relatively small, scenarios E and F are often almost similar.

The modeled sediment deposits for sediment removal scenarios A–F, applied to sediment distribution 1 (see Fig. 7), is visualized in Fig. 12. Little changes occur for scenarios A–C (removing sediment with D=2, 6, and 11 μm). The modeled sediment composition also changes little. Since the median grain size D_{50} of the suspended load is 10 μm, more than half of the sediment consists of these three fractions. Apparently, these fractions contribute little to the overall deposition rates. Deposition rates obviously decrease for scenario D, and are lowest for scenarios E and F. These latter two also generate a substantial fining of the sediment deposits.

Evaluating scenarios A–F for the other sediment distributions (2 and 3, see Fig. 7) as well, again suggests that the impact of the original distribution is limited (Fig. 13). The modeled deposition rates for distributions 2 and 3 are within approximately 20 % of deposition rates computed with scenario 1. Figure 13 also suggests that deposition on the upper flat is most strongly reduced for scenario D, while the lower flat is most strongly impacted by scenario F. Overall, E and F result in a similar reduction in deposition rate. This is more clearly illustrated by visualizing the relative decrease (Fig. 14). For the upper intertidal zone, the reduction in deposition rate is 50 % for scenarios 1D and 2D, but as high as 60 % for scenario 3D. Since deposition rates are still considerable on the lower intertidal zone, the average reduction for the entire intertidal zone is less than 20 % for scenario D. Highest impacts occur for scenarios E and F: here the reduction is more than 50 %. The reason for the cross-sectionally varying impact of the different scenarios is the cross-shore sediment distribution. The upper intertidal zone primarily consists of fine silt (see Figs. 9 and 12), and therefore a reduction in fine silt (scenario

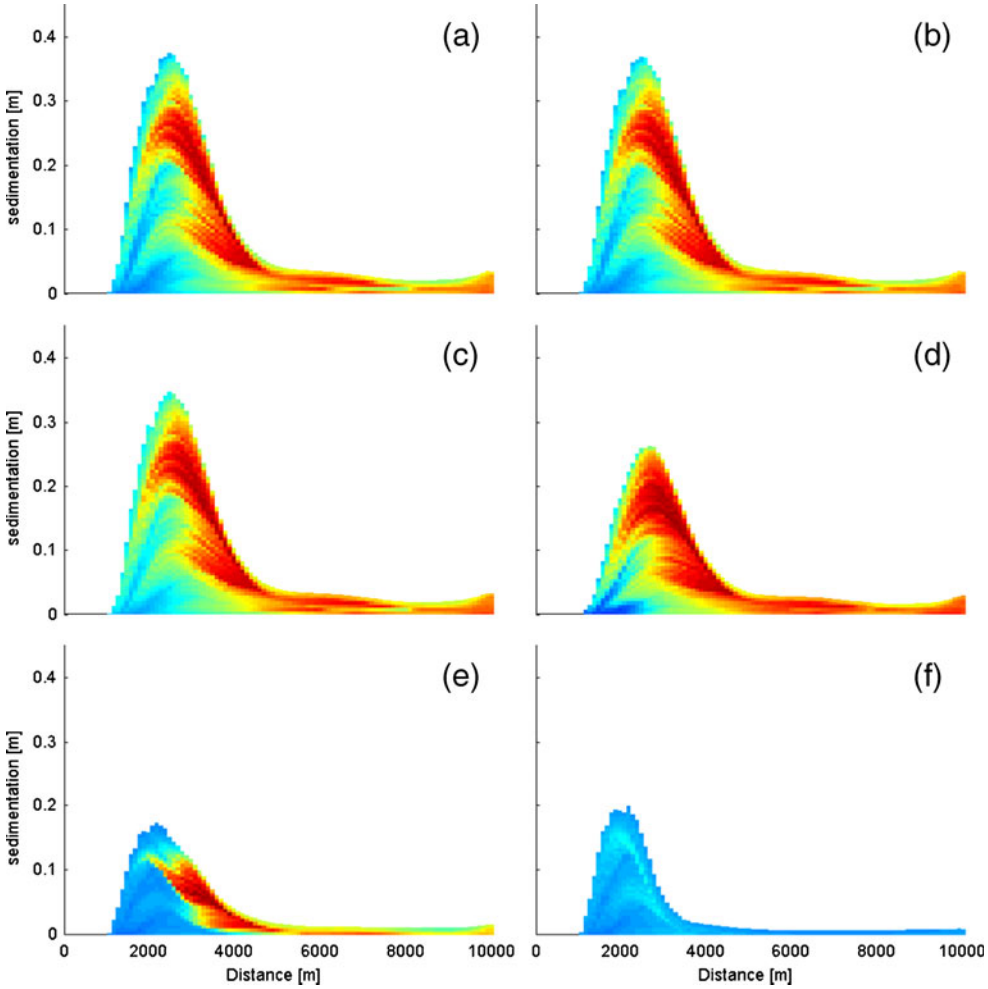

Fig. 12 Sediment composition after 90 days, using sediment distribution 1, without clay (2 μm, scenario A) (**a**), very fine silt (6 μm, scenario B) (**b**), *middle left* with fine silt (11 μm, scenario C) (**c**), *middle right* without fine-medium silt (18 μm, scenario D) (**d**), *lower left* without medium silt (33 μm, scenario E) (**e**), and *lower right* without coarse silt (58 μm, scenario F) (**f**), respectively. See the colorbar in Fig. 9b for grain size

D) will impact this area. The lower intertidal zone consists of coarser silt, and is therefore more strongly influenced by a decrease in coarse silt supply (scenarios E and F).

5 Discussion

5.1 Model limitations and modeled processes

Both the processes that shape tidal flats, and the shape of the flats themselves, are strongly simplified with the adopted modeling approach. Below we will briefly assess the implication of these shortcomings. The most pronounced shortcoming of the 2DV approach applied here is that both river flow and tidal filling generate strong currents in an along-flat direction in the Yangtze estuary. Only the seaward facing flats are dominated by local tidal filling and emptying. However, these seaward facing flats experience the highest deposition rates, and are therefore the main interest in this study. The limitations resulting from the process formulations are discussed below.

The morphology of tidal channels and flats strongly depends on sediment resuspension by wind waves (Fagherazzi et al. 2007; Fagherazzi 2010). Waves resuspend sediments, thereby generating an upflat-increasing sediment concentration, which in combination with tidal diffusion, creates an offshore-directed sediment flux. However, in the Yangtze estuary a distinct separation exists between periods in time where sediment dynamics are tide dominated, and a period in time where both waves and tides play an important role. The results presented here are mainly valid for the non-storm season. The importance of waves for resuspension can be estimated from data collected by Shi et al. (2011) on the Chongming tidal flat in September, during moderate tidal conditions (halfway spring to neap) and with onshore winds with a velocity twice the annual average. They computed bed shear stress due to waves, currents (τ_c), and combined waves currents using van Rijn (1993) (τ_{cw_vr93}) and Soulsby (1995) (τ_{cw_s95}). Over five tidal cycles, mean values of τ_{cw_vr93} and τ_{cw_s95} where 24.8 and 30.8 % (respectively) larger than τ_c. However, tidally maximum values of τ_{cw_vr93} and τ_{cw_s95} where only 7.6 and 19.2 % (respectively) larger than τ_c since

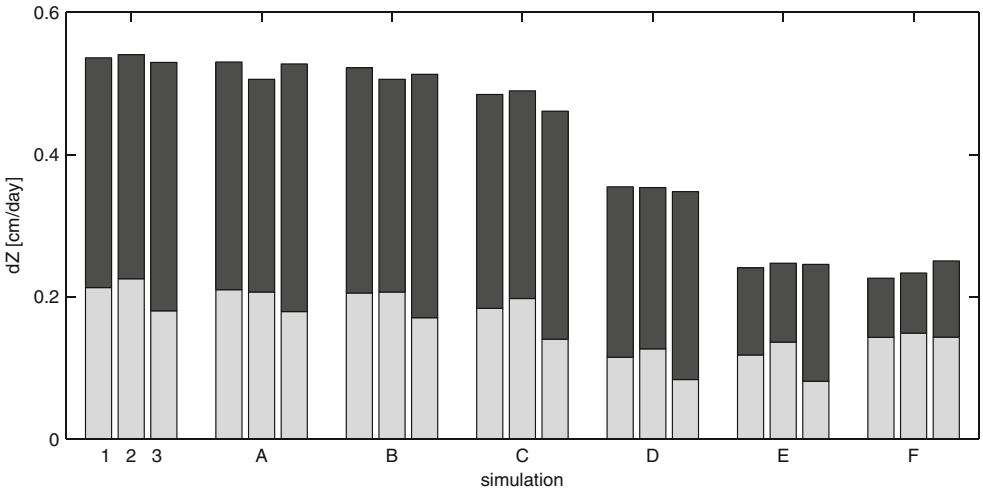

Fig. 13 Average deposition rate for 90 days in the intertidal zone for sediment distributions 1, 2, and 3 and scenarios A–F (each for sediment distribution 1, 2, and 3). *Dark grey* is deposition in the lower intertidal zone (below MSL) while *light gray* is deposition in the upper intertidal zone (above MSL). Note that the average deposition rate is not equal to the summation of both or the average (since the lower intertidal zone is large due to the concave profile)

peaks in bed shear stress were mainly current-driven. During spring tides, the role of waves on bed shear stress will therefore be even lower. Since our model was setup for conditions without waves (January–May) and with largest bed level changes occurring during spring tide, a tide-only model is concluded to be sufficiently accurate.

Flocculation and consolidation processes are not included: sediment is modeled as quartz particles which do not flocculate and form a rigid bed upon deposition. Field observations in the Yangtze Estuary (He et al. 2004, 2008; Guo and He 2011; Shao et al. 2011) reveal that sediment does flocculate and therefore tidal flat deposition will be, to some extent, influenced by cohesive processes (flocculation and consolidation). Van Ledden et al. (2004) concluded that the transition from non-cohesive to cohesive behavior (at least for erosion) occurs at a mud content of 10 %, a value confirmed to apply for silt-dominated sediment mixtures as well (te Slaa et al. 2013). Consolidation of silt-sized quartz particles as observed by Roberts et al. (1998) is probably pseudo-consolidation, resulting from pore water dissipation (te Slaa et al. 2013).The clay content on the Yangtze flats varies spatially, with the flats facing the open sea and the Yangtze River (Chongming and Jiuduansha) having a clay content less than 10 % (Yang 1998; Te Slaa et al. 2013). The effect of adding flocculation processes to the model would probably be increased deposition of the clay and fine silt fraction, little of which now settles on the tidal flats. Properly accounting for cohesive processes could therefore be part of future work. Nevertheless, since the TGD (and other dams) have comparatively small impact on fine-grained sediments (clay and very fine silts), excluding flocculation processes is not expected to substantially influence the predicted impact of large reservoirs.

Thirdly, fine-grained sediments may, in even relatively moderate sediment concentrations (several hundreds of

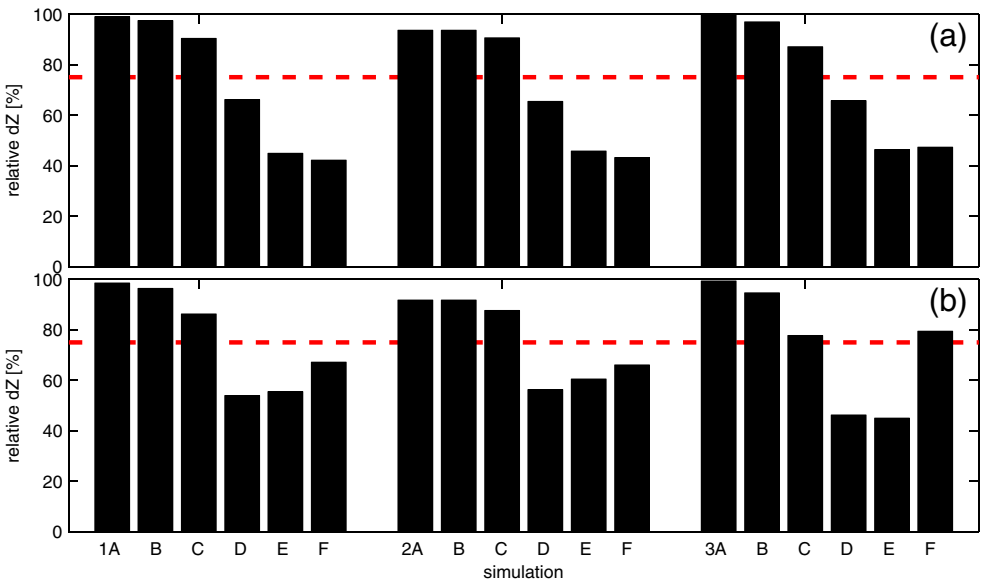

Fig. 14 Reduction in average deposition rate in the intertidal zone for sediment distributions 1, 2, and 3 and scenarios A–F, for the whole intertidal zone (**a**) and the upper intertidal zone (**b**). The reduction in sediment load is illustrated with the *red dashed line*

milligrams per liter), generate vertical concentration gradients sufficiently high to dampen turbulent mixing (Winterwerp 2001). Van der Ham and Winterwerp (2001) concluded that this damping of turbulent mixing by sediment-induced density stratification, leading to rapid deposition during decelerating flows, is an essential aspect of tidal flat sedimentation. However, using this feedback would also require modeling of waves, because at the concentrations modeled here the tide-induced turbulence is too low (except during spring tide) to overcome the sediment-induced buoyancy effects.

Finally, vegetation plays an important role in trapping sediment in the upper intertidal zone (Yang 1998; Yang et al. 2008; Li and Yang 2009), which is not modeled here. As a result the modeled deposition rate in the upper flat is too low and the grain size too high.

5.2 Deposition on the Yangtze tidal flats

As already noted by Yang et al. (2008), the deposition rates on the Yangtze flats are an order of magnitude higher than intertidal areas in NW Europe and North America (e.g., Pethick 1992; Callaway et al. 1997; Boorman et al. 1998; Esselink et al. 1998; Temmerman et al. 2004; Cahoon et al. 2006). In this section, we will explain these large deposition rates.

The most obvious reason is the large concentration: with an average sediment concentration of 0.4 g/l the Yangtze flats are relatively turbid. Deposition rates on tidal flats are strongly determined by the offshore sediment supply (Pritchard and Hogg 2003), implying deposition rates should be larger than average. However, even an average concentration of 0.4 g/l does not explain the order of magnitude difference in deposition rates.

Van Maren and Winterwerp (2013) concluded that in fine-grained areas shaped by cross-shore tidal flows, sediment is mainly transported toward the intertidal zone by the mixing lag (i.e., a time lag related to the time needed to vertically mix sediment), while within the intertidal zone sediment is transported further landward by the settling lag. The effectiveness of the settling lag is strongly related to the settling velocity w_s of the sediment particles, with highest landward transport rates for w_s=0.5 to 1 mm/s. For lower w_s, sediment does not settle at HW while for higher w_s the sediment transport rates become too low (and sediment does not reach the upper intertidal zone). A settling velocity of 0.5 to 1 mm/s corresponds to medium fine silt (18 μm) to medium silt (33 μm). The sensitiveness of deposition rates to these sediment fractions is further substantiated by the Yangtze tidal flat model. Hence, intertidal areas with a large supply of fine to medium silt in suspension (such as the Yangtze) can be expected to rapidly accrete.

Transport by the settling is not only determined by sediment properties: net transport and deposition can only occur in combination with a hydrodynamic asymmetry (van Maren and Winterwerp 2013). An important hydrodynamic asymmetry, already identified by Postma (1954, 1961, 1967) and van Straaten and Kuenen (1957, 1958), is a landward decreasing velocity amplitude. Such a spatial velocity gradient is most pronounced for a concave profile, resulting in much larger deposition rates compared with linear or convex tidal flat geometries (van Maren and Winterwerp 2013). Fine-grained coastal environments with a substantial amount of wave energy typically have a concave-upwards profile while tide-dominated tidal flats are typically convex upward (i.e., Kirby 2000). On the Yangtze flats, wave-dominated (erosional) processes dominate for a specific period over tide-dominated (depositional) processes, resulting in a concave-upward tidal flat profile. During periods of tide-dominated deposition, a pronounced horizontal velocity gradient exists (resulting from the concave profile), effectively transporting fine-grained sediments landward.

A second hydrodynamical condition of the Yangtze estuary, favoring high deposition rates, is tidal asymmetry. Postma (1954, 1961) and van Straaten and Kuenen (1957, 1958) focused on the importance of slack tide asymmetry for deposition on intertidal flats, and therefore this type of asymmetry is often associated with tidal flat deposition. However, van Maren and Winterwerp (2013) concluded that maximum flow asymmetry with $(2\phi_{M_2}-\phi_{M_4}) = 90°$ is much more effective for tidal flat deposition than slack tide asymmetry $(2\phi_{M_2}-\phi_{M_4}) = 180°$. Roberts et al. (2000) and Pritchard et al. (2002) also concluded that maximum flow asymmetry strongly contributes to net deposition rates on tidal flats. With a flood-dominant tide with $(2\phi_{M_2}-\phi_{M_4}) = 72°$, deposition rates on the Yangtze flats are partly high because of maximum flow asymmetry.

Conclusively, the deposition rates on the tidal flats of the Yangtze are exceptionally large due to the high sediment concentration, the abundance of silty material, the seasonal dominance of waves (shaping a concave profile), and the offshore tidal asymmetry.

5.3 Impact of dams on grain size distribution and downstream morphology

Dams may impact the downstream morphology by a changing discharge regime (Chen et al. 2010) and by retention of sediment. For reservoirs where the reservoir capacity is large with respect to the river discharge, the downstream river discharge will then be strongly influenced. For rivers with strongly varying river discharge and seasonality, the downstream morphology will be substantially changed by changes in discharge regime. This is the case in the Yellow River (e.g., van Maren et al. 2011). The discharge of the Yangtze River is much larger, and despite the great storage capacity of the TGD, it is insufficiently large to strongly

modify the discharge regime. Hence, the main impact of the TGD is related to retention of sediment in the reservoir.

The modeled scenarios strongly suggest that the impact of dams on coastal morphology is strongly influenced by the type of sediment that deposits inside the reservoirs. With a sediment concentration reduction of 25 %, the deposition rates may be reduced as much as 60 % (scenario E, with preferential trapping of sediment with D=33 μm). Although the model results cannot be directly extrapolated to large-scale intertidal flat dynamics, they do show that deposition rates will decline at a greater rate than the total suspended load, when preferentially silt is trapped. Even more, net changes in bed level are often a delicate balance between deposition rates and erosion rates, and therefore a 60 % decrease in deposition may lead to even larger net profile changes.

At present, the grain size of the suspended load entering the estuary is increasing (Datong, see Fig. 2c): from 9.3 μm in 1987–2002 to 10.3 μm in 2003–2010. Unfortunately, the collected data do not contain size distributions. It is therefore not possible to determine to what extent any change in grain size are caused by reductions in silt, sand and clay: a reduction of fine silt (D=10 μm) would not change the median grain size of the suspended load when D_{50}=10 μm. Additionally, the effect of dams on downstream estuary or deltas is often obscured by the buffering capacity of the river in between and the river mouth itself, and because of local human activities (such as land reclamations and construction of jetties). The river length between the main reservoir (the TGD) and the estuary head is 1,700 km, but due to the large transport capacity and limited availability of silt in the river bed, silt may be relatively rapidly (years to one to two decades) depleted. Nevertheless, the impact of silt trapping on the estuary is delayed for a limited period.

However, there is a large amount of silt present within the Yangtze estuary itself, not only on the extensive tidal flats, but also within the ETM, and in the subaqueous delta off the river mouth (Luo et al. 2012). Sediment is exchanged between the flats and the subtidal channel, especially during storm conditions (Yang et al. 2003b). The aerial extent of the Yangtze ETM is very large; extending several tens of km in seaward direction and from the Chongming Island down to Hangzhou Bay (see Han et al. 2006). With a water depth around 10 m and a sediment concentration of 0.5 g/l, this constitutes a sediment mass around 10 million ton. This is only a fraction (less than one tenth) of the annual reservoir deposition rates, and therefore sediment in the ETM itself is not an important sediment buffer. A larger sediment stock is the subaqueous delta. Sediment in the ETM is probably in equilibrium with the sediments deposited (previously) on the delta front: the subaqueous delta is presently eroding 75 million tons/year (compared with accumulation of >150 million tons/year before 1977; see Yang et al. 2011). Also a large amount of sediment is available south of the Yangtze Estuary, where suspended sediment concentrations are higher than the Yangtze ETM (see, e.g., Chen et al. 2003; Li et al. 2011; Ying et al. 2012). Nevertheless, after some time also the sediment in the ETM will decline, and then the effect of the upstream reservoirs (notably the TGD) will have an increasing impact on the downstream flats. Because of the dominance of silt in the Yangtze estuary, the fractional reduction of tidal flat deposition rates may be higher than the fractional trapping of the total sediment load in the upstream reservoir.

Although the present study focuses on the Yangtze River, we expect that the conclusions formulated here will be similar for river systems found elsewhere. For instance, the large trapping of sediment in the Yellow River strongly impacts the downstream morphology (van Maren et al. 2011) to the extent that the once silt-dominated river now has a median grain size over 100 μm (unpublished data Yellow River Conservancy Commission). The rate at which the downstream morphology (such as intertidal flats or the fluvial river bed) will be impacted by reservoir deposition depends not on the total reduction, but on the reduction of the sediment type dominating specific downstream morphology. We therefore encourage to systematically monitor not only sediment quantities (as is presently done), but also sediment type (both transported in suspension and within the river bed and on the estuarine flats).

6 Conclusions

The sediment load of the Yangtze River is decreasing. This decline, pre-dating the TGD but significantly accelerated since its construction, has been well documented in scientific literature. The TGD traps sand and silt while some clay is flushed through the reservoir. Sediment is eroded from the Yangtze River downstream of the reservoir. However, silt is limitedly available on the Yangtze River bed, and it is expected that most silt will be removed within a decade. Since silt is the dominant sediment type on the estuarine tidal flats, preferential trapping of silt may lead to larger reductions in coastline accretion (or even to erosion) than based on reductions of the total sediment load.

In order to better understand and quantify the sediment exchange mechanisms between the Yangtze and its tidal flats, a strongly schematized intertidal flat deposition model has been setup. This model broadly reproduces the typical deposition rates and patterns observed on the tidal flats and reveals that the observed deposition rates are exceptionally large due to the high sediment concentration, the abundance of silt, the seasonal dominance of waves (shaping a concave profile) and the offshore tidal asymmetry.

Experimenting with several scenarios exemplifying reservoir-induced changes in sediment concentration

revealed that deposition rates on the flats will be marginally influenced by a reduction of clay and fine silt. However, deposition rates may significantly decrease when median to coarse silt is removed from the suspended sediment load.

The work presented here stresses that the downstream estuarine morphology is not so much influenced by the total amount of sediment trapped in reservoirs, but especially by the trapped quantities of sediment dominating the downstream morphology. Mostly sand and silt are trapped in reservoirs, but since silt is transported in greater quantities than sand, the resulting morphologic adjustments are more rapid in silt-dominated morphologies than in their sandy equivalents. The downstream morphologies of silt-dominated rivers such as the Yangtze River and the Yellow River will therefore be more strongly impacted than sand-bed rivers.

Acknowledgments This work has been carried out as part of the Sino-Dutch collaboration project 'Effects of human activities on the eco-morphological evolution of rivers and estuaries' funded by the Dutch Academy of Social Sciences. It has also been supported by the Natural Science Foundation of China (41130856). The constructive comments of two anonymous reviewers are greatly appreciated.

References

Boorman LA, Garbutt A, Barrratt D (1998) The role of vegetation in determining patterns of the accretion of salt marsh sediment. In: Black KS, Paterson DM, Cramp A (eds) Sedimentary processes in the intertidal zone. Special Publication, Geological Society of London, pp 389–399

Cahoon DR, Hensel PF, Spencer T, Reed DJ, McKee KL, Saintilan N (2006) Coastal wetland vulnerability to relative sea-level rise: wetland elevation trends and process controls. In: Verhoeven JTA, Beltman B, Bobbink R, Whigham DF (eds) Wetlands and natural resource management. Ecological studies, vol 190. Springer, Heidelberg, pp 271–292

Callaway JC, Delaune RD, Patrick WH (1997) Sediment accretion rates from four coastal wetlands along the Gulf of Mexico. J Coast Res 13:181–191

Chen JY, Zhu HF, Dong YF, Sun JM (1985) Development of the Changjiang Estuary and its submerged delta. Cont Shelf Res 4:47–56

Chen SL, Zhang G, Yang SL (2003) Temporal and spatial changes of suspended sediment concentration and resuspension in the Yangtze River estuary. J Geogr Sci 13(4):498–506

Chen JY, Cheng HQ, Dai ZJ (2006) Harmonious development between utilization and protection of tidal flat and wetland—a case study in Shanghai area. In: Proceedings of the Second Int. Conf. on Estuaries and Coasts. Guandong Economy Publishing House, Guangzhou, China. ISBN 7-80728-422-6/P.2

Chen ZY, Wang Z, Finlayson B, Chen J, Yin D (2010) Implications of flow control by the Three Gorges Dam on sediment and channel dynamics of the middle Yangtze (Changjiang) River, China. Geology 38(11):1043–1046. doi:10.1130/G31271.1

Edmonds DA, Slingerland RL (2009) Significant effect of sediment cohesion on delta morphology. Nat Geosci 3:105–109

Esselink P, Dijkema KS, Reents S, Hageman G (1998) Vertical accretion and profile change in abandoned man-made tidal marshes in the Dollard estuary, the Netherlands. J Coast Res 14:570–582

Fagherazzi AMP (2010) Sediments and water fluxes in a muddy coastline: interplay between waves and tidal channel hydrodynamics. Earth Surf Proc Land 35:284–293

Fagherazzi S, Palermo C, Rulli MC, Carniello L, Defina A (2007) Wind waves in shallow microtidal basins and the dynamic equilibrium of tidal flats. J Geophys Res 112:F02024. doi:10.1029/2006JF000572

Fan D, Li CX (2002) Rhythmic deposition on tidal flats in the mesotidal Changjiang Estuary, China. J Sediment Res 72(4):543–551

Fan D, Guo Y, Wang P, Shi JZ (2006) Cross-shore variations in morphodynamic processes of an open-coast mudflat in the Changjiang delta, China: with an emphasis on storm impacts. Cont Shelf Res 26:517–538

Friedrichs CT, Aubrey DG (1988) Non-linear tidal distortion in shallow well-mixed estuaries: a synthesis. Estuar Coast Shelf Sci 27:521–545

Fuggle R, Smith W (2000) Large dams in water and energy resource development in the People's Republic of China (PRC). Country review paper prepared as an input to the World Commission on Dams, Cape Town. http://www.dams.org

Geleynse N, Storms JEA, Walstra DJR, Jagers HRA, Wang ZB, Stive MJF (2011) Controls on river delta formation; insights from numerical modelling. Earth Planet Sci Lett 302(1–2):217. doi:10.1016/j.epsl.2010.12.013

Guo L, He Q (2011) Freshwater flocculation of suspended sediments in the Yangtze River, China. Ocean Dyn 61:371–386

Han Z, Jin Y–Q, Yun CX (2006) Suspended sediment concentrations in the Yangtze River estuary retrieved from the CMODIS data. Int J Remote Sens 27(19):4329–4336

He Q, Yu ZY, Wang YY, Yun CX (2003) Field measurements of surface sediment concentration in the Yangtze Estuary, China. In: Proc. Of the Int. Conf. on Estuaries and Coasts, Hangzhou, China, November 2003

He Q, Cheng J, Wang YY (2004) In situ estimates of floc size and settling velocity in the Changjiang Estuary. In: Proceedings of Ninth International Symposium on River Sedimentation, Yichang, China, pp 416–422

He Q, Tang J, Cheng J (2008) A study of in situ floc size in turbidity maximum, Yangtze Estuary, China, In: Sediment and Ecohydraulics,: INTERCOH 2005, T Kusada, H Yamanishi, J Spearman, J. Gailiani (ed), Elsevier, p. 287–294

Hu K, Ding PX, Wang ZB, Yang SL (2009) A 2D/3D hydrodynamic and sediment transport model for the Yangtze Estuary, China. J Mar Syst 77(1–2):114–136. doi:10.1016/j.jmarsys.2008.11.014

Kirby R (2000) Practical implications of tidal flat shape. Cont Shelf Res 20:1061–1077

Kuang C, Liu X, Gu J, Guo Y, Huang S, Liu S, Yu W, Huang J, Sun B (2013) Numerical prediction of medium-term tidal flat evolution in the Yangtze Estuary: impacts of the Three Gorges project. Cont Shelf Res 52:12–26

Le Hir P, Roberts W, Cazaillet O, Christie M, Bassoullet P, Bacher C (2000) Characterization of intertidal flat hydrodynamics. Cont Shelf Res 20:433–459

Lesser GR, Roelvink JA, van Kester JATM, Stelling GS (2004) Development and validation of a three-dimensional morphological model. Coast Eng 51:883–915

Li H, Yang SL (2009) Trapping effect of tidal marsh vegetation on suspended sediment, Yangtze Delta. J Coast Res 25(4):915–924

Li Q, Yu M, Lu G, Cai T, Bai X, Xia Z (2011) Impacts of the Gezhouba and Three Gorges reservoirs on the sediment regime in the Yangtze River, China. J Hydrol 403:224–233

Luo XX, Yang SL, Zhang J (2012) The impact of the Three Gorges Dam on the downstream distribution and texture of sediments

along the middle and lower Yangtze River (Changjiang) and its estuary, and subsequent sediment dispersal in the East China Sea. Geomorphology 179:126–140

Mastbergen DR, van den Berg JH (2003) Breaching in fine sands and the generation of sustained turbidity currents in submarine canyons. Sedimentology 50:625–637

Pawlowicz R, Beardsley B, Lentz S (2002) Classical tidal harmonic analysis including error estimates in MATLAB using T_TIDE. Comput Geosci 28:929–937

Pethick JS (1992) Saltmarsh geomorphology. In: Allen JRL, Pye K (eds) Saltmarshes: morphodynamics. Conservation and engineering significance. Cambridge University Press, Cambridge, pp 41–62

Postma H (1954) Hydrography of the Dutch Wadden Sea. Ph.D. thesis, Groningen University, 106 p

Postma H (1961) Transport and accumulation of suspended matter in the Dutch Wadden Sea. Neth J Sea Res 1:148–190

Postma H (1967) Sediment transport and sedimentation in the marine environment. Estuar Spec Publ 83:158–179

Pritchard D, Hogg AJ (2003) Cross-shore sediment transport and the equilibrium morphology of tidal flats under tidal currents. J Geophys Res 108(C10):3313. doi:10.1029/2002JC001570

Pritchard D, Hogg AJ, Roberts W (2002) Morphological modelling of intertidal mudflats: the role of cross-shore tidal currents. Cont Shelf Res 22(11–13):1887–1895. doi:10.1016/S0278-4343(02)00044-4

Roberts J, Jepsen R, Gotthard D, Lick W (1998) Effects of particle size and bulk density on erosion of quartz particles. J Hydraul Eng 124:1261–1267

Roberts W, Le Hir P, Whitehouse RJS (2000) Investigation using simple mathematical models of the effect of tidal currents and waves on the profile shape of intertidal mudflats. Cont Shelf Res 20:1079–1097

Saito, Y (2001) Deltas in Southeast Asia and East Asia: their evolution and current problems. In: Proc. APN/SURVAS/LOICZ Joint Conference on Coastal Impacts of Climate Change and Adaptation in the Asia-Pacific Region, Kobe, Japan, 2000, pp 185–191

Shao YY, Yan YX, Maa JP (2011) In situ measurements of settling velocity near Baimao shoal in Changjiang estuary. J Hydraul Eng, March

Shi BW, Yang SL, Wang YP, Bouma TJ, Zhu Q (2012) Relating accretion and erosion at an exposed tidal wetland to the bottom shear stress of combined current–wave action. Geomorphology 138(1):380–389. doi:10.1016/j.geomorph.2011.10.004

Soulsby RL (1995) Bed shear stresses due to combined waves and currents. In: Stive MJF, De Vriend HJ, Freds+e J, Hamm L, Soulsby RL, Teisson C, Winterwerp JC (eds) Advances in coastal morphodynamics. An overview of the G-8 Coastal Morphodynamics Project. Delft Hydraulics, Delft, the Netherlands, pp 420–423

Syvitski JPM, Kettner AJ, Hannon MT, Hutton EWH, Overeem I, Brakenridge GR, Day J, Vörösmarty C, Saito Y, Giosan L, Nicholls RJ (2009) Sinking Deltas. Nat Geosci 2:681–689

Te Slaa S, He Q, Van Maren DS, Winterwerp JC (2013) Sedimentation processes in silt-rich sediment mixtures. Ocean Dyn 63:399–421. doi:10.1007/s10236-013-0600-x

Temmerman S, Govers G, Meire P, Watel S (2004) Simulating the longterm development of levee-basin topography on tidal marsh. Geomorphology 63:39–55

Van der Ham R, Winterwerp JC (2001) Turbulent exchange of fine sediments in a tidal channel in the Ems/Dollard estuary, part II: analysis with a 1DV numerical model. Cont Shelf Res 21:1629–1647

Van Ledden M, van Kesteren WGM, Winterwerp JC (2004) A conceptual framework for the erosion behaviour of sand–mud mixtures. Cont Shelf Res 24(1):1–11

van Maren DS (2007) Grain size and sediment concentration effects on channel patterns of silt-laden rivers. Sediment Geol 202:297–316

van Maren DS, Winterwerp JC (2013) The role of flow asymmetry and mud properties on tidal flat sedimentation. Continent Shelf Res. doi:10.1016/j.csr.2012.07.010

van Maren DS, Winterwerp JC, Wu BS, Zhou JJ (2009a) Modelling hyperconcentrated flow in the Yellow River. Earth Surf Process Landf 34:596–612

van Maren DS, Winterwerp JC, Wang Z-Y, Pu Q (2009b) Suspended sediment dynamics and morphodynamics in the Yellow River, China. Sedimentology. doi:10.1111/j.1365-3091.2008.00997.x

van Maren DS, Yang M, Wang ZB (2011) Predicting the morphodynamic response of silt-laden rivers to water and sediment release from reservoirs: lower yellow river, China. J Hydraul Eng 137:90–99

van Rijn LC (1993) Principles of sediment transport in rivers, estuaries and coastal seas. Aqua Publications, Amsterdam, the Netherlands, p 64

van Rijn LC (2007) A unified view of sediment transport by currents and waves, part 1: initiation of motion, bed roughness and bed load transport. J Hydraul Eng 133:649–667

Van Straaten LMJU, Kuenen PH (1957) Accumulation of fine grained sediments in the Dutch Wadden Sea. Geol mijnbouw 19:329–354

Van Straaten LMJU, Kuenen PH (1958) Tidal action as a cause of clay accumulation. J Sediment Petrol 28(4):406–413

Vörösmarty CJ, Meybeck M, Fekete B, Sharma K, Green P, Syvitski JPM (2003) Anthropogenic sediment retention: major global impact from registered river impoundments. Global and planetary change, vol 39. Elsevier, Amsterdam, pp 169–190

Walling DE (2009) The impact of global change on erosion and sediment transport by rivers: current progress and future challenge. WWDR scientific paper. The United Nations Educational, Scientific and Cultural Organization, Paris

Wang ZQ, Chen ZY, Li MT, Chen J, Zhao YW (2009) Variations in downstream grain-sizes to interpret sediment transport in the middle-lower Yangtze River, China: a pre-study of Three-Gorges Dam. Geomorphology 113:217–229

Winterwerp JC (2001) Stratification effects by cohesive and non-cohesive sediment. J Geophys Res 106(C10):22.559–22.574

Xu J (2007) Trends in suspended sediment grain size in the upper Yangtze River and its tributaries, as influenced by human activities. Hydrol Sci 52(4):777–791

Xu K, Milliman JD (2009) Seasonal variations of sediment discharge from the Yangtze River before and after impoundment of the Three Gorges Dam. Geomorphology 104(3–4):276–283

Yang SL (1998) The role of scirpus marsh in attenuation of hydrodynamics and retention of fine sediment in the Yangtze Estuary. Estuar Coast Shelf Sci 47:227–233

Yang SL (1999) Sedimentation on a growing intertidal island in the Yangtze River Mouth. Estuar Coast Shelf Sci 49:401–410

Yang SL, Ding PX, Chen SL (2001) Changes in progradation rate of the tidal flats at the mouth of the Changjiang River, China. Geometry 38:167–180

Yang SL, Belkin IM, Belkin AI, Zhao QY, Zhu J, Ding XD (2003a) Delta response to decline in sediment supply from the Yangtze River: evidence of the recent four decades and expectations for the next half-century. Estuar Coast Shelf Sci 57:589–599

Yang SL, Friedrichs CT, Ding PX, Zhu J, Zhao QY (2003b) Morphological response of tidal marshes, flats and channels of the outer Yangtze River mouth to a major storm. Estuaries 26:1416–1425

Yang SL, Zhang J, Zhu J, Smith JP, Dai SB, Gao A, Li P (2005) Impact of dams on Yangtze River sediment supply to the sea and delta intertidal wetland response. J Geophys Res 110:F03006. doi:10.1029/2004JF000271

Yang Z, Wang H, Saito Y, Milliman JD, Xu K, Qiao S, Shi G (2006) Dam impacts on the Changjiang (Yangtze) River sediment discharge to the sea: the past 55 years and after the Three Gorges Dam. Water Resour Res 42, W04407. doi:10.1029/2005WR003970

Yang SL, Zhang J, Dai SB, Li M, Xu XJ (2007a) Effect of deposition and erosion within the main river channel and large lakes on sediment delivery to the estuary of the Yangtze River. J Geophys Res 112, F02005. doi:10.1029/2006JF000484

Yang SL, Zhang J, Xu XJ (2007b) Influence of the Three Gorges Dam on downstream delivery of sediment and its environmental implications, Yangtze River. Geophys Res Lett 34, L10401. doi:10.1029/2007GL029472

Yang SL, Li H, Ysebaert T, Bouma TJ, Zhang WX, Wang YY, Li P, Li M, Ding PX (2008) Spatial and temporal variations in sediment grain size in tidal wetlands, Yangtze Delta: on the role of physical and biotic controls. Estuar Coast Shelf Sci 77:657–671

Yang SL, Milliman JD, Li P, Xu K (2011) 50,000 dams later: erosion of the Yangtze River and its delta. Glob Planet Chang 75(1–2):14–20

Ying XM, Ding PX, Wang ZB, Van Maren DS (2012) Morphological impact of the construction of an offshore Yangshan deepwater harbor in the port of Shanghai, China. J Coast Res 28(1A):163–173

Zhang Z (2011) Quantifying the influence of Three Gorges Project on Yangtze suspended sediment flux, water discharge and water level. Dissertation for Master's Degree, East China Normal University, 53 pp